ELSEVIER

Journal of Power Sources 105 (2002) 189–194

JOURNAL OF POWER SOURCES

www.elsevier.com/locate/jpowsour

Button cell supercapacitors with monolithic carbon aerogels

H. Pröbstle*, C. Schmitt, J. Fricke

Physikalisches Institut der Universität Würzburg, Am Hubland, D-97074 Würzburg, Germany

Abstract

Carbon aerogels are highly porous materials prepared via pyrolysis of resorcinol–formaldehyde aerogels. The density of the aerogels can be varied in a wide range, whereby the major part of the pores is accessible to ionic conductors. Therefore, the application of high surface area aerogels as electrodes in supercapacitor devices is promising. In the present publication, the integration of thin monolithic aerogel composites in button cell casings is presented. The preparation of thin and mechanically stable aerogel electrodes was performed via integration of carbon fibers into the aerogel skeleton. In order to increase the external electrode area in the button cells (volume: 2.1 cm^3) a special folding technique for the electrodes (thickness: 180 μm) was employed. The aerogel capacitors exhibit an excellent long term stability with no significant degradation after 80,000 charging and discharging cycles. According to a ragone-evaluation of the impedance data, the maximum power output and energy content for the aerogel button cells are 4.6 W and 4.9 mWh, respectively. The influence of CO_2-activation on the capacitive and resistive behavior of the electrodes in different aqueous electrolytes is analyzed using innovative analytical methods for cyclic voltammetry and impedance spectroscopy.

Keywords: Carbon aerogel; Electrodes; Fiber-reinforced; Supercapacitors; Button cells

1. Introduction

Supercapacitors are electrochemical double-layer capacitors with moderate energy and high power densities. Their field of application extends from back-up power storage devices to peak power sources for electrical vehicles. From the permanent growth of announced supercapacitor patents in recent years an outstanding growing market in the field of supercapacitors can be predicted. From a total market of $ 200 million in 1998 supercapacitor sales are estimated to approach $ 11 billion by 2015 including consumer, industrial and automotive applications [1]. A survey of the state of development and of the applied materials for these devices is given in [2,3]. Among various high surface area carbon blacks used as electrodes in supercapacitors carbon aerogels represent a promising and innovative material. Their monolithic structure enables the manufacture of binderless electrodes. The porosity and pore size distribution of the material can be varied in a wide range which renders it suitable for supercapacitors and fuel cells [4–6]. In using oxidative treatments the capacitive behavior of aerogel electrodes can be further improved. While gas phase oxidation increases the surface area and widens the pores [7,8], electrochemical oxidation introduces capacitive enhancing redox groups on the carbon surface [9,10]. A modification of the aerogels is the integration of fibers or clothes in the sol–gel-precursor which enables the manufacture of thin and mechanically stable monolithic aerogels films with thickness in the range of several 100 μm [11]. Especially supercaps for high power density applications require such electrodes with a low resistance.

2. Experimental and measurement techniques

2.1. Electrode preparation

The manufacture of the aerogel electrodes has been performed according to the following procedure: resorcinol (R) was dissolved in formaldehyde (F) in a molar ratio of 1:2. Subsequently, sodium carbonate (C) was added as catalyst. The amount of catalyst (R/C-ratio) allows to control the size of the primary particles. The density of the RF-gels was adjusted by varying the concentration of water in the sol [12]. After immersing a carbon cloth in the RF-sol, the polymerization was performed at three temperatures (30, 50, and 90 °C). The resulting cloth reinforced RF-gels were dried subcritically with respect to acetone and pyrolysed in an argon atmosphere at 800 °C. In Fig. 1 a SEM micrograph of the cloth-reinforced aerogel structure is shown. The crevices in the material are caused by the shrinkage of the RF-gel which is embedded in the non-shrinking carbon fiber matrix. The crevices are useful in procedures or applications which require a highly accessible pore

* Corresponding author.

0378-7753/02/$ – see front matter
PII: S0378-7753(01)00938-7

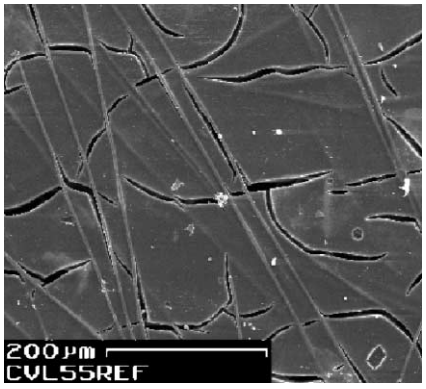

Fig. 1. SEM micrograph of a non-activated cloth-reinforced aerogel (thickness: 180 μm, density: 0.544 g/cm^3). The stripes are the carbon fibers integrated in the aerogel.

structure, such as vapor phase activation procedures and low resistive surface accessibility with electrolytes. In order to reduce the electrolyte resistance further the aerogel composites were activated in controlled CO_2 atmosphere at 950 °C as described in [8].

2.2. Integration in button cells

Before integrating the aerogels in button cells they were impregnated in 4 M KOH in vacuum to exclude adsorbed gases from the inner pore volume. KOH served as electrolyte since use of sulfuric acid with it's excellent conductivity is not compatible with the Ni-coated button cell casing. An effective arrangement of the aerogel electrodes in button cell casings has been reached with the folding technique shown in Fig. 2.

Compared with the arrangement of two thick monolithic slices facing each other a lower cell resistance results from the enlarged external electrode area in the folded system. According to this, a single electrode area of 24 cm^2 made up of nine folded aerogel slices with a thickness of 180 μm was integrated into the button cells with a volume of 2.1 cm^3. The current collector used in this system consists of a corrosion resistant stainless steel foil (thickness: 25 μm); the separator was made of cellulose. In order to reduce the contact resistance between aerogel and current collector, the aerogel slices were coated with Ni on one side.

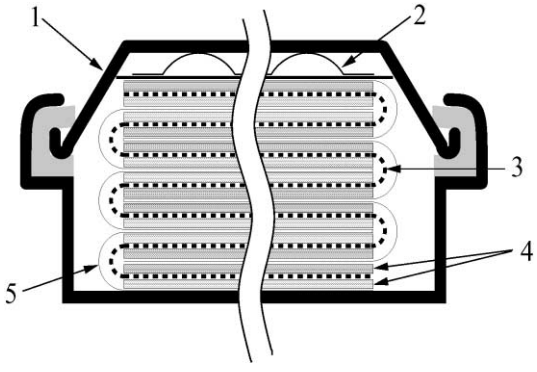

Fig. 2. Schematic of the applied folding technique. Indices—1: casing; 2: spring; 3: separator; 4: electrodes; 5: current collector.

2.3. Measurement techniques

In order to control the charging performance of the aerogel electrodes after activation impedance spectroscopy was applied to single circular aerogel slices with a diameter of 19 mm. The experiments were performed in a three electrode arrangement in 1 M sulfuric acid with an Ag/AgCl reference electrode system as described in [9]. The impedance data were evaluated by a Solartron FRA 1250 impedance analyzer under the control of a Solartron 1287 potentiostat. The applied voltage amplitude was 30 mV within a frequency range of 20 kHz–8.25 mHz. All impedance measurements were performed at open circuit potential.

The same impedance parameters were applied for the investigation of the button cells in a two electrode set-up whereby 4 M KOH served as electrolyte. In addition, long term cycling tests have been performed using cyclic voltammetry within the potentials of 0–1 V at a scan rate of 50 mV/s. The two electrode measurement was made employing a 363 EG&G potentiostat.

The surface areas and pore volumes of the non-activated and activated samples were derived via N_2 adsorption at 77 K using a Micromeritics ASAP 2000 apparatus [13,14].

2.4. Data evaluation

In Fig. 3, a complex plane plot for the impedance response of a button cell with integrated non-activated aerogel electrodes is shown. In addition, the corresponding plot of capacitance versus real part of the impedance (*RC*-plot) is shown. The capacitance (C) was derived from the imaginary part Z'' of the impedance according to

$$C = \left|\frac{1}{\omega Z''}\right|, \quad (1)$$

whereby ω denotes the angular frequency of the applied ac-signal. The *RC*-plot gives detailed information on the charging characteristics of the electrode. According to a theoretical treatise on the impedance response of porous electrodes, the ac-signal is increasingly propagating into inner pore sites of the electrode with decreasing frequencies [15]. The impedance data in region (a) in Fig. 3 account for this behavior. With decreasing frequency more inner pore sites and surface parts are involved which results in a higher capacitance. The propagation of the signal into inner pore structures includes longer electrolyte pathways, which results in an increasing real part of the impedance.

According to this the two distinct slopes in region (a) and (b) appearing in the *RC*-plot (Fig. 3) can be attributed to the propagation of the signal in two regions with different pore dimensions. In region (a) the propagation occurs along expanded pore structures (low resistance, high *C*/*R*-ratio).

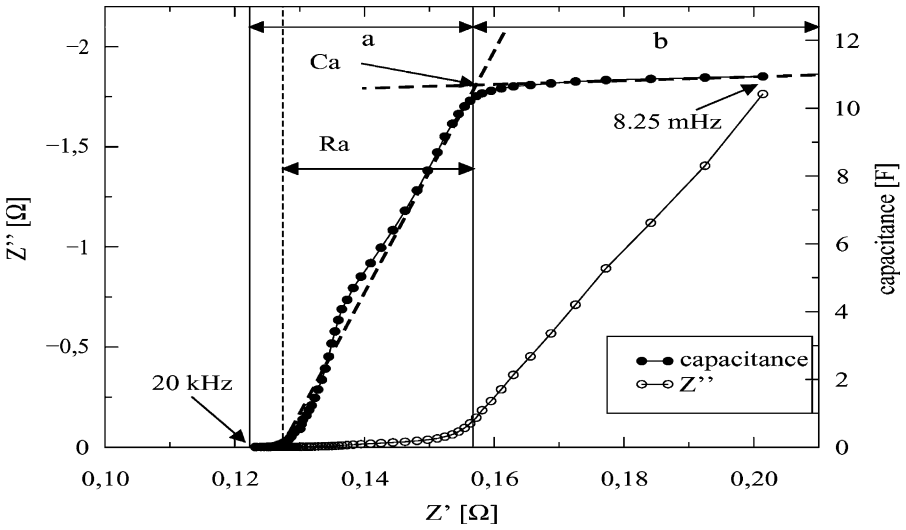

Fig. 3. Complex plane plot for the impedance of a button cell capacitor with fiber reinforced aerogel electrodes (imaginary part Z'' vs. real part Z'). In addition (right ordinate), the corresponding *RC*-plot (capacitance vs. real part of the impedance Z') is shown. The straight lines in region (a) and (b) denote different charging mechanisms in the electrode.

In contrast region (b) with a low *C*/*R*-ratio, where the typical constant phase element appears, can be ascribed to narrow pore dimensions and electrolyte pathways in the carbon particles (high resistance, low *C*/*R*). A detailed analysis of impedance data regarding structural data obtained from small angle X-ray scattering (SAXS) and N_2-sorption technique confirmed the microporous correspondence of the constant phase element in carbon aerogel electrodes [16].

Fig. 4 shows a cyclic voltammogram of an aerogel button cell. This technique was applied for long term characterization with up to 80,000 charge and discharge cycles of the systems. It allows to monitor faradaic degradation processes of current collector, casing and electrodes. In order to evaluate the total capacitance C and serial resistance R_s the equivalent circuit shown in Fig. 5 was used in a non-linear least squares fit procedure to the experimental data set. The corresponding fit function according to the circuit (Fig. 5)

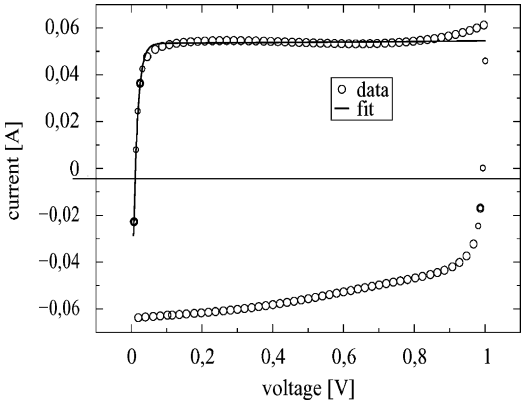

Fig. 4. Cyclic voltammogram with a scan rate of 5 mV/s of a button cell capacitor and the corresponding fit according to the circuit model in Fig. 5.

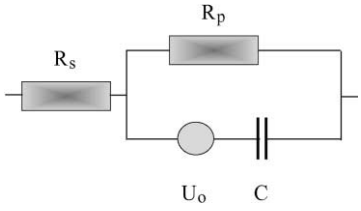

Fig. 5. Equivalent circuit model. R_s denotes serial contact and electrolyte resistances, R_p the self discharge resistance, C the capacitance of the electrode and U_o the residual voltage of the capacitor at the switching points 0 and 1 V, respectively.

was obtained using the Laplace representation. The basic requirement for the applicability of the model is the voltage source in series with the total capacitance of the cell. It takes into account the residual charge of the capacitor when switched between 0 and 1 V [17]. The corresponding fit results for the data in Fig. 4 are $R_s = 0.21\ \Omega$ and $C = 10.5$ F. These values correspond to the data derived from the *RC*-plot for the same cell in Fig. 3 at 8.25 mHz and confirm the applicability of the equivalent circuit model.

3. Results and discussion

In Fig. 6, *RC*-plots of non-activated and activated aerogel slices are shown. The physical data of the samples derived from BET and electrochemical methods are summarized in Table 1.

The *RC*-plot reveals the optimized charging characteristics of the activated electrode. A rise in total capacitance at 8.25 mHz as well as a reduction of the low frequency resistance is observed. The latter effect can be explained by the larger micropore volume after activation which

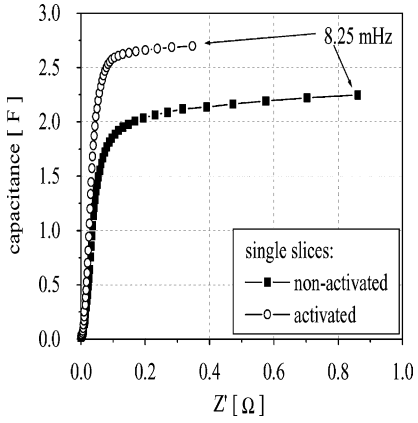

Fig. 6. *RC*-plot of aerogels derived with three electrode measurements in 1 M H_2SO_4 (see Table1). Resistive and inductive effects in the high frequency region have been eliminated.

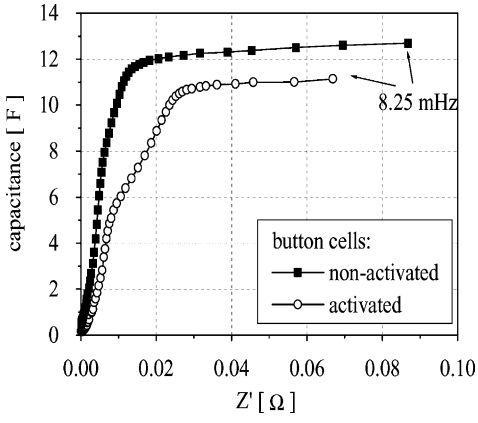

Fig. 7. *RC*-plot of button cells with activated and non-activated electrodes. For technical data see Table 2. Resistive and inductive effects in the high frequency region have been eliminated.

introduces wider electrolyte pathways in the carbon particles (see Table 1). The higher surface area of the activated electrode accounts for additionally created micropores which increase the capacitance [7,8]. This tendency is enforced by the build-up of various capacitance enhancing surface groups, e.g. quinone/hydroquinone groups, during CO_2-activation. The corresponding cyclic voltammogram of the activated sample in sulfuric acid revealed significant reversible redox peaks between 0.5 and 1 V versus Ag/AgCl, respectively [9].

The performance of the electrodes is changed if the electrode materials are integrated into button cells with 4 M KOH as electrolyte. The corresponding data are plotted in Fig. 7. A comparison with Fig. 6 reveals that the expected rise in capacitance for the activated cell is obviously suppressed in the KOH system. Both the higher resistance and lower capacitance in the main capacitive region (compare region (a) in Fig. 3) of the activated system indicate a reduced accessibility of the pores in the KOH system.

These results can be attributed to the insufficient wetting of the carbon surface with KOH observed especially for the activated aerogel system. After impregnation in vacuum for several hours adsorbed gases were still present on the pore surface of the electrodes. Since adsorbed gases reduce the electrolyte content in the electrode a higher charging resistance appears in the main capacitive region of Fig. 7. The reduced pore accessibility reduces the active surface area as well resulting in a lower capacitance compared to the non-activated electrode.

Another reason for the reduced performance of the activated electrode in KOH is the absence of pseudocapacitances. The typical quinone/hydroquinone redox peaks observed with CO_2-activated aerogels in sulfuric acid were not present in the corresponding cyclic voltammogram of the KOH system.

In Figs. 8 and 9 the long term cycling performance of the activated and non-activated aerogel cap is shown. The data were derived according to the model sketched in Fig. 5. The resistance data represent the total serial resistance of the cells including the contribution of contacts, carbon skeleton and separator.

Taking into account the standard deviation of the data (5% for the capacitance, 2% for the resistance) no significant

Table 1
Physical data of the activated and non-activated aerogel slice plotted in Fig. 6[a]

	Non-activated	Activated
Density (g cm^{-3})	0.544	0.468
Thickness (μm)	180	180
External area (cm^2)	2.8	2.8
BET surface area (m^2 g^{-1})	534	923
Micropore volume (cm^3 g^{-1})	0.13	0.27
Volumetric capacitance (F cm^{-3})	44.1	52.9
Specific electrolyte resistance (Ω cm^2)	2.44	0.98

[a] The electrochemical data were derived at 8.25 mHz from the impedance data in 1 M H_2SO_4. The specific electrolyte resistance was evaluated according to $\rho_{spec.} = Z'$ (8.25 mHz) × (external electrode area).

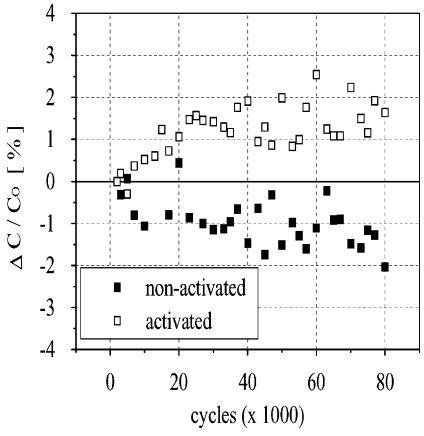

Fig. 8. Relative change in total capacitance during long term cycling tests for the activated and non-activated button cell. The data have been evaluated according to Fig. 5.

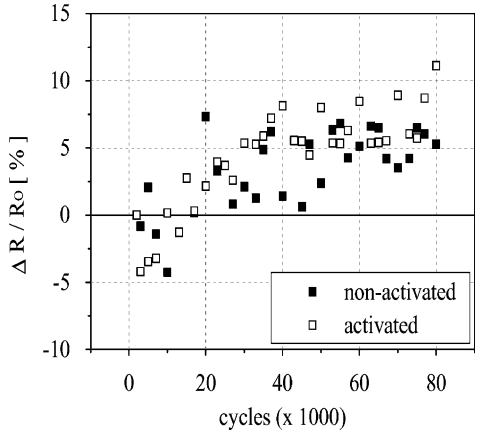

Fig. 9. Relative change in serial resistance during long term cycling tests for the activated and non-activated button cell.

degradation appears in the non-activated system. This confirms the electrochemical stability of all components like electrolyte, current collector and aerogel electrode within the applied voltage range.

Since both cells are identical, except for the electrode material, the increase in resistance in the activated system can be contributed to the activated electrode. The slight rise in capacitance and resistance of the cell accounts for an additional wetting of surface structures during the cycling tests. As another reason, gas forming surface reactions at the roughened and chemically modificated activated carbon surface could result in a higher load resistance of the capacitor.

In Table 2, the performance data of the investigated button cells are summarized. The lower energy content of the activated system reflects the reduced surface accessibility and capacitance of the activated electrodes as discussed above. The discrepancy of the ESR at high frequency is the reason for the strongly varying maximum power output of the cells. The ESR at 20 kHz reflects the contact quality between aerogel slices and current collector as well as the resistance of the current collector.

Table 2
Performance data of the activated and non-activated button cells[a]

	Non-activated cell	Activated cell
Total mass (g)	7.67	7.58
Electrode mass (g)	0.49	0.40
Maximum power output (W)	4.6	2.7
Maximum energy content (mWh)	4.9	4.2
Total capacitance (F)	12.7	11.1
ESR (20 kHz) (mΩ)	77	130
ESR (8.25 mHz) (mΩ)	160	200

[a] The electrochemical data were derived at 8.25 mHz from the impedance data. The energy content and power output of the cells have been evaluated according to the ragone-transformation of the impedance data with a cell voltage of 1.2 V as described in [18].

Another contribution to the ESR is the electrolyte resistance in the separator which was estimated to be 20 mΩ. If current collector and contact effects are neglected, the maximum power output at high frequencies for the non-activated cell would increase from 4.6 to 18 W. This higher performance could be roughly achieved with a bipolar arrangement of electrodes with the same external area as for the button cells (24 cm^2).

In order to extend the performance of the button cells with activated electrodes further experiments regarding both pseudocapacitance-supporting electrolytes, i.e. substitutes for sulfuric acid, and highly conductive current collectors have to be performed.

4. Conclusion

An innovative folding technique for the integration of thin monolithic carbon aerogels in button cell casings was developed. The performance data of the button cell supercapacitors are promising and show almost no degradation after 80,000 charging and discharging cycles. The performance of such cells could be further optimized if CO_2-activated electrodes with pseudocapacitance-supporting electrolytes were used which are compatible with the Ni-coated button cell casing. According to this the specific electrolyte resistance could be further reduced up to 60% with an increase in capacitance up to 20% compared to non-activated electrodes.

References

[1] J. Nickerson, in: Proceedings of 9th International Seminar on Double Layer Capacitors and Similar Energy Storage Devices, Deerfield Beach, FL, 1999.
[2] B.V. Tilak, C. Chen, Electrochem. Soc. Proc. 95–29 (1995) 111.
[3] B.E. Conway, Electrochemical Supercapacitors, Kluwer Academic Publishers/Plenum Press, New York, 1999.
[4] R.W. Pekala, et al., J. Non-Cryst. Solids 225 (1998) 74.
[5] R. Saliger, U. Fischer, C. Herta, J. Fricke, J. Non-Cryst. Solids 225 (1998) 81.
[6] R. Leuschner, M. Lipinski, R. Petričević, J. Fricke, Intern. Patent #WO99/27597.
[7] R. Saliger, H. Pröbstle, G. Reichenauer, J. Fricke, in: P. Vincencini (Ed.), Proceedings of the 9th CIMTEC. Part L. Innovative Materials in Advanced Energy Technology, 1999.
[8] R. Saliger, G. Reichenauer, J. Fricke, in: K.K. Unger, G. Kreysa, J.P. Baselt (Eds.), Studies in Surface Science and Catalysis, Vol. 128, Elsevier, Amsterdam, 2000, p. 381.
[9] H. Pröbstle, R. Saliger, J. Fricke, in: K.K. Unger, G. Kreysa, J.P. Baselt (Eds.), Studies in Surface Science and Catalysis, Vol. 128, Elsevier, Amsterdam, 2000, p. 371.
[10] K. Kinoshita, Carbon: Electrochemical and Physicochemical Properties, Wiley, New York, 1988.
[11] R. Petričević, M. Glora, J. Fricke, Planar Fibre Reinforced Carbon Aerogels for Application in PEM Fuel Cells, Carbon, submitted for publication.
[12] R.W. Pekala, F.M. Kong, J. Phys. Colloq. C (Paris) 4 (1989) 33.
[13] F. Rouquerol, J. Rouquerol, K. Sing, Adsorption by Powders & Porous Solids, Academic Press, London, 1999.

[14] K. Kaneko, C. Ishii, M. Ruike, H. Kuwabara, Carbon 30 (1992) 1075.
[15] R. de Levie, in: P. Delahay (Ed.), Advances in Electrochemistry and Electrochemical Engineering, Vol. 6, Interscience, New York, 1967, p. 329.
[16] H. Pröbstle, J. Fricke, The Physical Correspondence of the Constant Phase Element in Microporous Carbon Electrodes, in: Proceedings of the 198th Meeting of the Electrochemical Society, Phoenix, 2000, submitted for publication.
[17] R. Paul, Elektrotechnik und Elektronik für Informatiker I, Teubner, Stuttgart, 1994.
[18] T. Christen, M.W. Carlen, C. Ohler, in: Proceedings of the 9th International Seminar on Double Layer Capacitors and Similar Energy Storage Devices, Deerfield Beach, FL, 1999.